EURASIAN PHYSICAL TECHNICAL JOURNAL

2024, Volume 21, No.3 (49)

Special Issue

https://doi.org/10.31489/2024No3/117-124

Received: 22/05/2024 Revised: 22/06/2024 Accepted: 23/09/2024 Published online:30/09/2024

Original Research Article

UDC 53.093

INFLUENCE OF MOISTURE CONDITION AND SILICA SAND ON FRICTION COEFFICIENT OF WIND TURBINE BRAKE SYSTEM

Mohammed O.A.[1], Mohammed S.A. [1], Ghazaly N.M.*[2,3]

[1] Department of Mechanical Engineering, College of Engineering, University of Mosul, Mosul, Iraq.

[2] Technical College, Imam Ja'afar Al-Sadiq University, Baghdad, Iraq.

[3] Department of Mechanical Engineering, South Valley University, Qena, Egypt.

*Corresponding author: nouby.ghazaly@eng.svu.edu.eg

Abstract. *Major drive train parts for the horizontal wind turbines including the gearbox, generator, and brake system have very high repair and replacement costs and take a long time to complete. This paper investigates the impact of environmental air pollution on drivetrain tribology behaviors. Experimental research of the wind turbine's drive train system is simulated and investigated. The mechanical brake system of wind turbines is the subject of one case study chosen for this research paper. This research paper is examined how impurities affect the friction coefficient of the brake on wind turbines. According to the findings, the friction coefficient rises with each increase in wind turbine shaft speed. Also, it has been discovered that the size of the contaminants' particles significantly affects the friction coefficient. Furthermore, the findings may offer helpful insights of the drive train system that as humidity increased from 30 mm^3 to 90 mm^3, the coefficient of friction significantly decreased.*

Keywords*:* wind turbines; moisture condition; silica sand; friction coefficient.

1. Introduction

Recently, the global use of power has tripled, in large part due to economic expansion. While developed countries like the United States, Japan, and Europe still require more electricity production to keep up with their higher consumption levels and to satisfy the expanding number of applications, Egypt's ongoing economic growth has resulted in a significant increase in the demand for electricity. The need for alternatives to finite fossil fuels and their negative environmental effects has propelled the wind industry's explosive growth during the last 20 years. A wind turbine design needs to undergo advanced engineering analysis to further increase the cost effectiveness of wind turbines, both in terms of dependability and the design of larger turbines as well as overall cost effectiveness. From several angles, it is possible to examine the cost effectiveness in the wind turbine sector. One of the biggest problems in this industry is the high maintenance costs and unproductive downtime caused by faults and failures in the functioning drive train components including bearings, gearboxes, and couplings, as cited by B. Lu et al., 2009 [6] and K.K. Borum et al., 2006 [12]. Also, many researchers including Alex Alsyouf I. and El-Thalji I., 2008 [1], H. Peng et al., 2023 [20] reported that the mechanical reliability of wind turbine-based renewable electricity generation has unique challenges when compared to utility-scale fossil fuel-based power. Due to the sheer number of turbines and their dispersion, maintenance is a challenging and infrequent undertaking, and peak loads—due to unstable winds and grid faults as well as challenging environmental factors like temperature swings and moisture lead to excessive operation. Thus, one of the more difficult current practical tribological problems is presented by wind turbine systems. The actuators and drivetrain of the turbine have experienced costly repairs due to contact failures in gear and bearing components.

Maalawi K.Y. and Badr M.A. 2023 [14], Babu B.C., Mohanty K.B. 2010 [4] mentioned that the primary mechanical parts of the system are housed in the wind turbine's exterior housing, or nacelle. These components include the power electronics, the generator, bearings, the rotor shaft, the gearbox unit, the filtering system for lubricants, the mechanical braking mechanism, and the brakes, as shown in Figure 1. The generator is driven by the high-speed shaft, which receives energy from the main shaft via the gearbox. The nacelle cover and drivetrain parts are attached to a bedplate, It sits atop of a yaw mechanism which actively points the rotor toward the wind.

Despite the wide range of wind turbine powertrain types now in use, utility-scale systems typically fall into one of three groups as described by Q. Sun et al., 2002 [18]. The first idea entails employing two bearings to support the primary shaft. Radial loads are carried by the bearing closest to the gearbox, whereas loads axial and radial are carried by the bearing closest to the rotor. The primary shaft therefore solely sends torque to the gearbox. Torque arms can be added to the gearbox unit to transfer response torque to the bedplate since the gearbox may direct reaction torque in that direction Randall, R.B. and J. Antoni 2011 [19], Y. Amirat et al., 2007 [24]. The second idea, referred to as a "three-point suspension" design, an axial bearing is used to support the primary shaft close to the rotor, while the opposite end of the shaft can be support by a radial bearing from inside the gearbox. The actual gearbox is supported by two torque arms and positioned on the bed plate. The gearbox is directly integrated into the nacelle in the third category of drivetrain. This design incorporates all rotor support bearings into the gearbox, which also receives all rotor load inputs. Although this design can be viewed as favorable for reducing the weight of the nacelle., compatibility issues between the gearbox and the other nacelle components may cause early failure as mentioned by B. Lu et al., 2009 [6], A. Staino, B. Basu 2013[2], Peng Guo and David Infield 2012 [17].

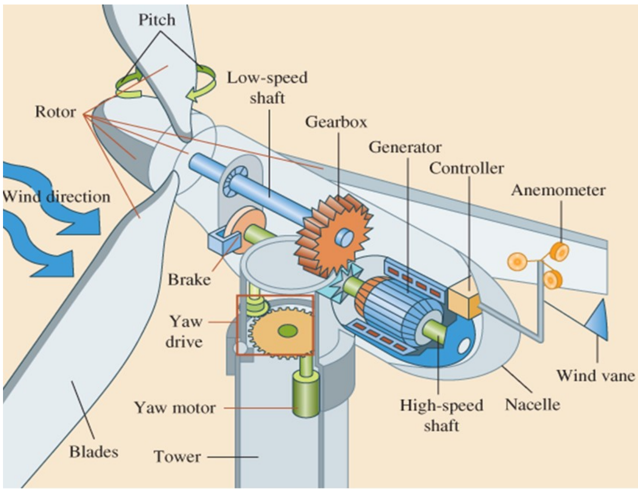

Fig.1. A horizontal-axis wind turbine's main part.

The high-speed portion of the powertrain of contemporary wind turbines typically includes a mechanical brake between the gearbox and the generator. The major function of this mechanical brake, which is nearly always shaped like a disc brake, is to shut off the rotor when it is shutting down in order to perform maintenance and repair work. Some turbines use the mechanical brake as a supplementary braking method in addition to serving as a parking brake so that aerodynamic braking can be used as well. In order to reduce the size and weight of the brake disc in larger wind turbines, the mechanical brake is located on the gearbox's high-speed side. The mechanical brake may reduce a gearbox's dependability because it is mounted on a high-speed shaft. When the vehicle is at rest, the braking loads often collide with the wind turbulence forces, causing minute oscillatory movements of the gear teeth. As a result of these movements, the gear teeth may wear as found in M. Ragheb et al., 2011 [15], Gasch, R. and J. Twele 2012 [8], Sørensen, J. D. et al., 2011, Bhutta, et al., 2012 [5].

Howell R, et al., 2010 [10], Nadica Stojanovic, et al., 2022 [16], Zhang et al., 2023 [25] reported that the cutting and grinding from manufacturing, as well as internally induced wear wrench age, metal oxide corrosion products, airborne abrasives entering through vents, and mechanical seals are other sources of contaminated particles. Additionally, to particle pollution, Lubricating and hydraulic fluids also contain trace amounts of water that dissolve. Depending on the base stock and additions. The saturation level (maximum dissolved water content) is normally between 300 and 500 ppm. Also, Leung DY and Yang Y 2012 [13], Roman, et al., 2022 [21] showed that the free water, which collects in the system's low points, is defined as water contamination that exceeds the saturation limit. Depending on the amount, A bout 1 lm worth of emulsified free water droplets are remained suspended in the oil, giving it a hazy to milky appearance. Sources of water include liquid water acquired during transit and storage as well as humidity entering through vents and mechanical seals as mentioned by Roy Saha 2015 [22], Islam, M.R. et al., 2013 [11], G. Yu, et al., 2011 [9], Belhocine and Nouby, 2015 [3], Chellaganesh Durai, et al., 2021 [7].

According to the previously described discussions, fabrication of a new drivetrain test system to assess the tribology behaviors of wind turbine is conducted. The effect of contaminates on the tribology behaviors of the wind turbine brake system is studied. The effects of various-sized sand particles as pollutants is investigated. In additions, the humidity as water spray on the mechanical brake system are examined under different speeds and several loads.

2. General Description of Bearing Test-rig

As depicted in Figure 2, a sophisticated test apparatus is created to capture precise and trustworthy data which are utilized to assess gearbox performance by utilizing a variety of signal processing methods. The major goal of these experimental research is to keep an eye on how an automobile gearbox is performing at various speeds. A 100 mV/g-sensitivity piezoelectric accelerometer is mounted on the casing to provide vibration signatures of gearboxes. AC motor of A 7.5 kW power with a variable speed controller and a maximum speed of 1500 rpm makes up the drive unit. A tachometer S119-LT photo-type with 0.1 rpm resolution is used to detect the rotational speed directly. The type of bearings used is ball bearings, where they are positioned between brake assembly and motor, and the brake mechanism is connected to the AC motor by a mild steel shaft. A control valve-equipped hydraulic braking system is employed in order to enforce the necessary load and show its value on a pressure gauge.

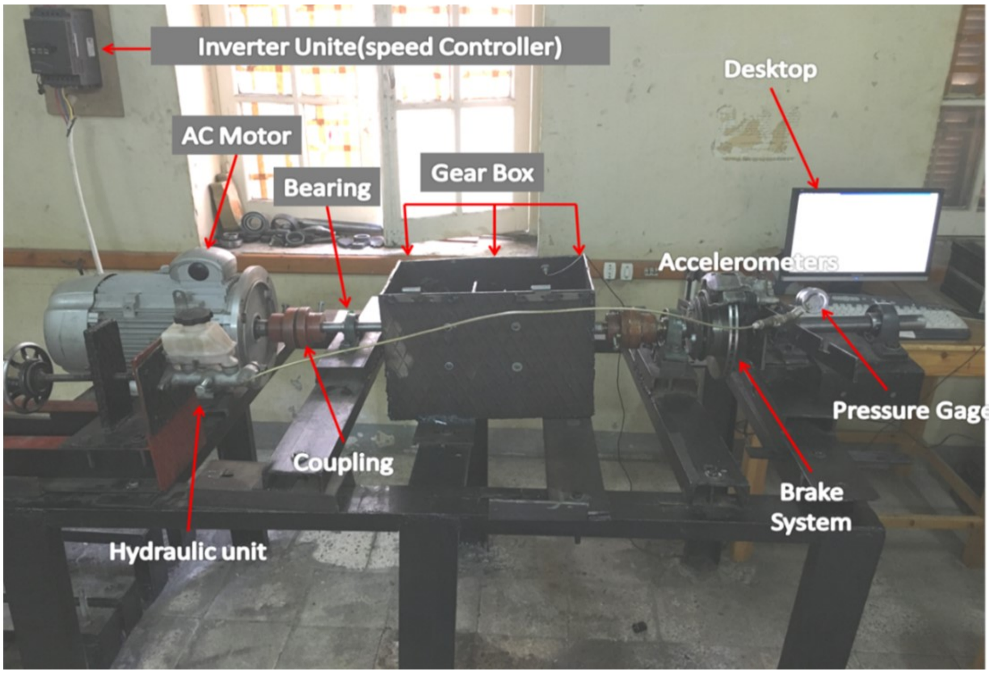

Fig.2. Test rig of wind turbine's drive train system

To collect the vibration information, a magnetic base is used to mount a piezoelectric accelerometer directly above the gearbox. The accelerometer's output signal is received by the dual channel vibration analyzer, which saves it as vibration signatures. Using PULSE software and a connection linked to a computer, the vibration analyzer's recorded data can be retrieved. The data Acquisition System that used is 3560-B Brüel & Kjaer Vibro-Acoustics type. To get reference signatures, the gearbox is tested without any load. The test rig's vibrations are recorded and confirmed prior to the experiment in order to determine whether there is a misalignment. To stabilize the vibration, the setup is run for 15 minutes.

3. Results and Discussion

This section defines the drive train system as the electromechanical component of a wind turbine that transmits mechanical power from the rotor hub to the electric power generator. It consists of shafts, bearings, gearboxes, shaft couplings, mounts, mechanical brake systems, and other functional components. This system is crucial to the tribology of wind turbines. The mechanical braking system is chosen so that the impact of impurities on friction coefficient, a key determinant of tribology behaviors can be studied. The investigation of the brake system uses actual disc brakes.

The high-speed section of the powertrain of contemporary wind turbines often has a mechanical brake, which is located between the gearbox and the generator. The main purpose of this mechanical brake during shutdown is to lock down the rotor so that maintenance and repair work may be done. It nearly always resembles a disc brake. Several turbines use the mechanical brake in addition to acting as a parking brake so that aerodynamic braking can be employed as well. The mechanical brake on larger wind turbines is located on the gearbox's high-speed side to reduce the brake disc's size and weight. Due to its placement on a high-speed shaft, the mechanical brake may make a gearbox less dependable. At rest, braking loads frequently clash with wind turbulence forces, causing minute oscillations in the gear teeth.

The experiment involved measuring the coefficient of friction once every second. Averaged over 60 seconds is the coefficient of friction. The friction coefficient varies over time while the testing is continuing because the metal-to-metal contact causes deformation on the contact surface. The coefficient friction stabilizes once the machine has been running. Figure 3 show the friction coefficient vs time for a wind shaft rotating at 1000 rpm and 10 bar of applied pressure. At dry, standard temperature, the friction coefficient is typically 0.35.

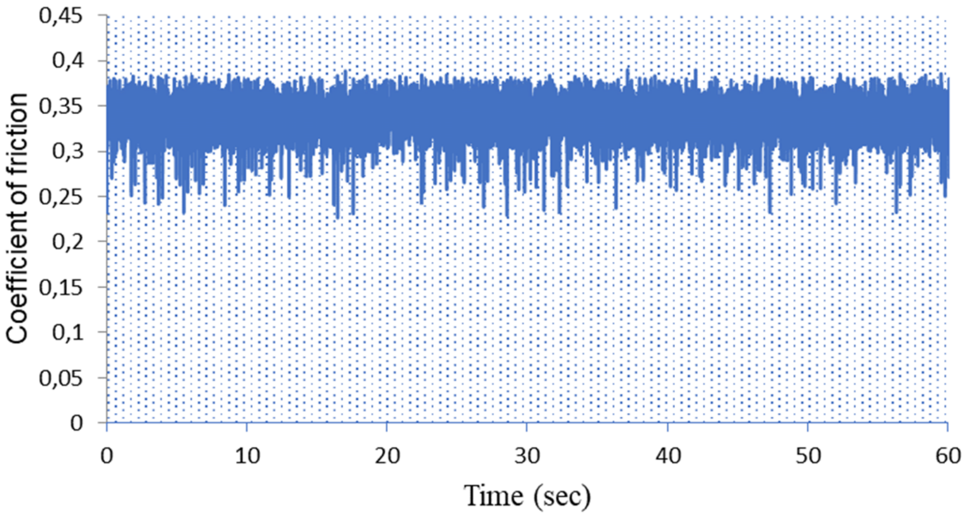

Fig.3. Variation over time of the friction coefficient at 1000rpm and 10 bar.

3.1 Effect of Silica Sand Particles on Wind Turbine Brake

When braking, both the brake rotor and the brake pads are exposed to weather environmental particles, which may have an impact on the surface quality of the brake pads in the form of moisture, humidity, or other impurities. Several vibration experiments are conducted to determine the effect of this particle on the brake friction coefficient. The effects of various-sized sand particles as pollutants on the mechanical brake system are examined. As indicated in Figure 4, this experiment used silica sand particles with a size range between 0 and 300 μm that are most frequently found in the weather. There were three different silica sand size ranges used: 0-100 µm, 100-200 µm, and 200-300 µm. On a brake test apparatus that is vertically oriented, the experiments are run at various sliding speeds and applied contact forces. The outcome demonstrates that the silica sand particles had an impact on the disc brake's surface behavior. The disc brake's silica sand particle friction coefficient results reveal a rougher surface region with several primary contact plateaus, wear scars, and groove structures with varying levels of roughness and sliding direction. Figure 4 shows a plot of the impact of tiny silica sand particles at various rotational speeds.

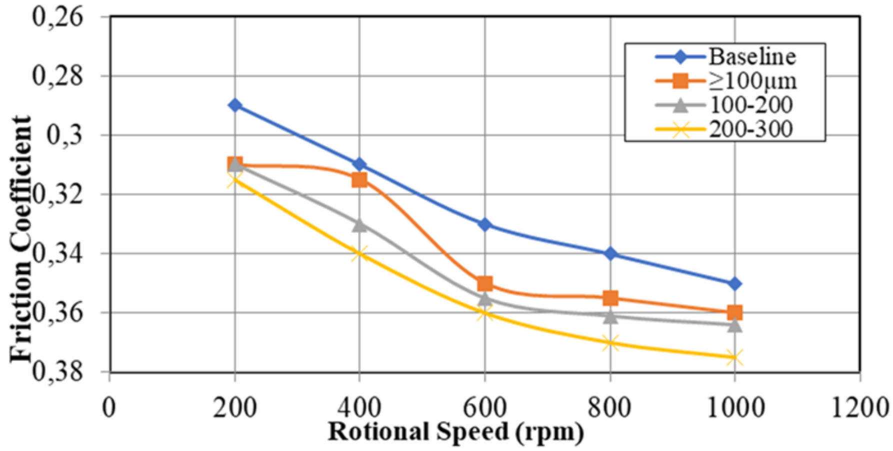

Fig.4. Effect small particles of silica sand with different rotational speed.

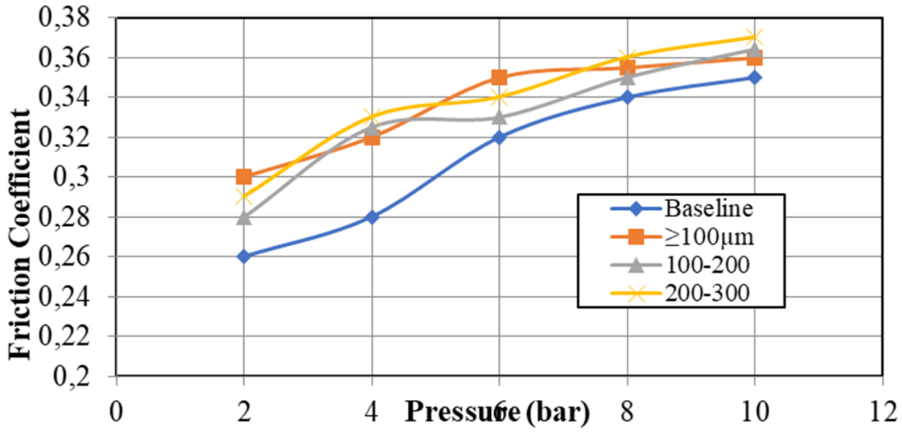

Fig.5. Effect small particles of silica sand with different brake pressure.

The results reveal that the friction coefficient is discovered to rise with every braking speed. Additionally, it has been discovered that the size of the particles significantly affects the friction coefficient. Figure 5 depicts the impact of tiny silica sand particles with various braking pressures on friction coefficient. The friction coefficient is discovered to rise with applied load. Additionally, it has been discovered that the particles' sizes significantly influence the friction coefficient, which rises as the load increases.

3.2 Influence of Moisture Condition on Friction Coefficient

As a quick technique to introduce the moisture condition, water was sprayed on the wind turbine mechanical braking system. This experiment demonstrated how humidity could affect the mechanical braking mechanism of a wind turbine. As the wind turbine shaft speed grew from 200 rpm to 1000 rpm, moisture is added to the friction, which significantly increased the coefficient friction. Additionally, it is demonstrated that as humidity increased at each speed from 30 mm^3 to 90 mm^3, there is a significant drop in coefficient friction.

The change in shear rate, which can affect the mechanical characteristics of the mating materials, may be the cause of the increase in coefficient of friction with an increase in rational speed. At larger shear strain rates, these materials' strength increases. However, in the dry test, the friction coefficient likewise increased when the speed was increased. Figure 6 depicts the impact of humidity on coefficient of friction as a function of rotational speed. Additionally, Figure 7 illustrates the impact of humidity on various braking pressures.

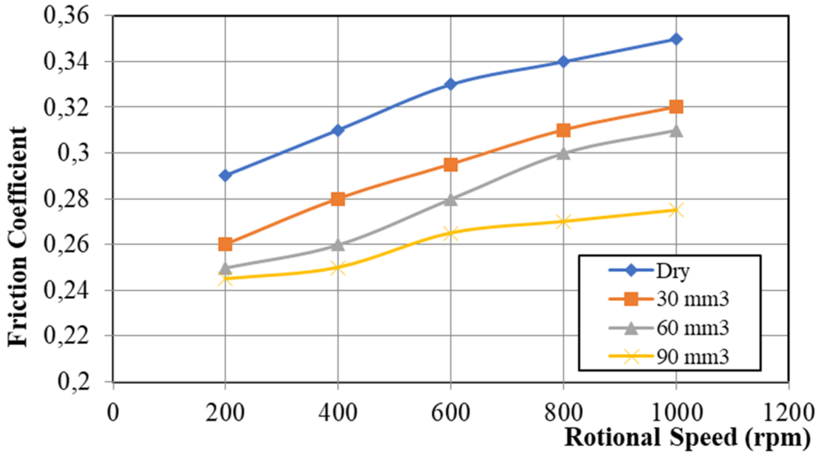

Fig.6. Effect humidity with different rotational speed.

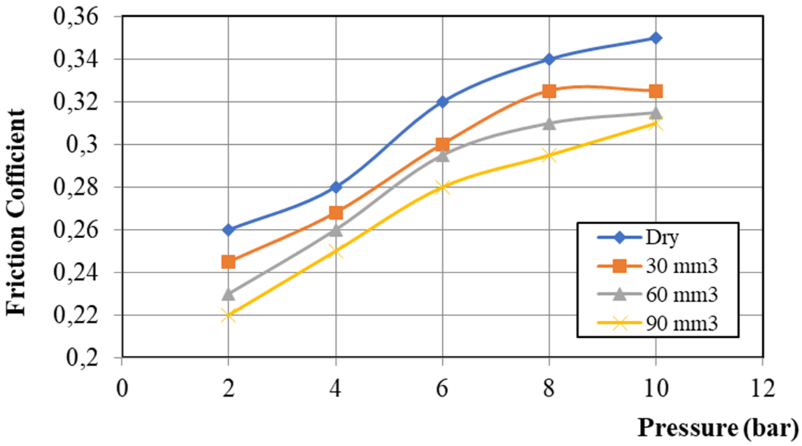

Fig.7. Effect humidity with different brake pressure.

4. Conclusions

From the experimental results indicate that humidity and silica sand under the braking speeds and load have a prominent influence on the wind turbine braking system. In additions, the following inferences can be made in light of the experimental findings:

1. The outcome demonstrates that the silica sand particles had an effect on the surface behavior of the wind turbine disc brake.
2. It has been discovered that friction coefficient rises with every wind turbine shaft speed.
3. The friction coefficient is shown to be significantly influenced by the particle size, and when the load on the wind turbine brake system grows, the friction coefficient also increases.

For each speed of wind turbine, it was demonstrated that as humidity increased from 30 mm^3 to 90 mm^3, the coefficient of friction significantly decreased.

Conflict of interest statement

The authors declare that they have no conflict of interest in relation to this research, whether financial, personal, authorship or otherwise, that could affect the research and its results presented in this paper.

CRediT author statement

Mohammed Omar A.: Conceptualization, Software; Mohammed; Sufyan A.: Writing - Review & Editing; Ghazaly Nouby M.: Supervision, Methodology. The final manuscript was read and approved by all authors.

References

1 Alsyouf I., El-Thalji I. (2008) Maintenance practise in wind power systems: a review and analysis. *Proceeding of the European Wind Energy Conference and Exhibition*, Brussels, Belgium, 2588 – 2597. https://www.proceedings.com/content/005/005469webtoc.pdf.

2 Staino A., Basu B. (2013) Dynamics and control of vibrations in wind turbines with variable rotor speed. *Enginnering Structures*, 58 – 67. DOI: 10.1016/j.engstruct.2013.03.014.

3 Belhocine A., Ghazaly N.M. (2015) Effects of Material Properties on Generation of Brake Squeal Noise Using Finite Element Method. *Latin American Journal of Solids and Structures,* 12, 2 (8). DOI:10.1590/1679-78251520.

4 Babu B.C., Mohanty K.B. (2010) Doubly-fed induction generator for variable speed wind energy conversion systems–modeling and simulation. *Int. J. Comput. Electr. Eng.,* 2(1), 141–147. DOI:10.7763/IJCEE.2010.V2.127.

5 Bhutta M.M.A., Hayat N., Farooq A.U., Ali Z., Jamil S.R., Hussain Z. (2012) Vertical axis wind turbine–A review of various configurations and design techniques. *Renewable and Sustainable Energy Reviews*, 16(4), 1926-1939. DOI: 10.1016/j.rser.2011.12.004.

6 Lu B., Li Y., Wu X., Yang Z. (2009) A review of recent advances in wind turbine condition monitoring and fault diagnosis. *IEEE Power Electron. Mach. Wind Appl.*, 1–7. DOI:10.1109/PEMWA.2009.5208325.

7 Chellaganesh Durai, M. Adam Khan, J. T. Winowlin Jappes, Nouby M. Ghazaly, P. Madindwa Mashinini (2021) Solid particle erosion studies on thermally deposited alumina– titania coatings over aluminium alloy. *International Journal of Minerals, Metallurgy and Materials,* 28, 1186–1193. DOI:10.1007/s12613-020-2099-8.

8 Gasch R., Twele J. (2012) Wind Power Plants - Fundamentals, Design, Construction and Operation, Springer. DOI:10.1007/978-3-642-22938-1.

9 Yu G., Shen X., Zhu X., Du X.Z. (2011) An insight into the separate flow and stall delay for hawt, *Renew. Energy,* 36 (1), 69–76. DOI: 10.1016/j.renene.2010.05.021.

10 Howell R., Qin N., Edwards J., Durrani N. (2010) Wind tunnel and numerical study of a small vertical axis wind turbine. *Renewable energy*, 35(2), 412-422. DOI:10.1016/j.renene.2009.07.025.

11 Islam M.R., Mekhilef S., Saidur R. (2013) Progress and recent trends of wind energy technology. Renew. Sustain. Energy Rev. *Renewable and Sustainable Energy Reviews,* 21, 456 – 468. DOI:10.1016/j.rser.2013.01.007.

12 Borum K.K., McGugan M., Brøndsted P. (2006) Condition monitoring of wind turbine blades. *Proc. of the 27th Risøe Intern. Symposium on Materials Science. Polymer Composite Materials for Wind Power Turbines*, 139–145. http://www.risoe.dk/rispubl/AFM/sympsale.htm

13 Leung D.Y., Yang Y. (2012) Wind energy development and its environmental impact: a review. *Renewable and Sustainable Energy Reviews*, 16(1), 1031-1039. DOI: 10.1016/j.rser.2011.09.024.

14 Maalawi K.Y., Badr M.A. (2003) A practical approach for selecting optimum wind rotors. *Renewable Energy,* 28, 803–822. DOI:10.1016/S0960-1481(02)00028-9.

15 Ragheb M., Ragheb A.M. (2011) Wind Turbines Theory - The Betz Equation and Optimal Rotor Tip Speed Ratio. *Fundam. Adv. Top. Wind Power*, 1(1). DOI:10.5772/21398.

16 Nadica Stojanovic, Ghazaly N.M., Grujic I., Doric J. (2022) Determination of Noise Caused by Ventilated Brake Disc with Respect to the Rib Shape and Material Properties Using Taguchi Method. *Transactions of FAMENA,* 46 (4). DOI:10.21278/TOF.464011219.

17 Guo P., Infield D. (2012) Wind turbine tower vibration modelling and monitoring by the non-linear state estimation technique. *Energies*, 5(12), 5279 – 5293. DOI:10.3390/en5125279.

18 Sun Q., Chen C., Zhang D., Xi F. (2020) Pattern recognition for automatic machinery fault diagnosis," *Mechanical Systems and Signal Processing*, 142, 106680. DOI:10.1016/j.ymssp.2020.106680.

19 Randall R.B., Antoni J. (2011) Rolling element bearing diagnostics—A tutorial, *Mechanical Systems and Signal Processing. 25*, 2, 485 – 520. DOI:10.1016/j.ymssp.2010.07.017.

20 Peng H., Li S., Shangguan L., Fan Y., Zhang H. (2023) Analysis of Wind Turbine Equipment Failure and Intelligent Operation and Maintenance Research. *Sustainability*, 15(10), 8333. DOI:10.3390/su15108333.

21 Roman A., Lemos, G.V.B., Gasparin A.L. (2022) Friction material wear: Effects and interactions between service brake temperature, lining contact pressure, and vehicle speed. *Proceedings of the Institution*

of Mechanical Engineers, Part J: Journal of Engineering Tribology, 236(12), 2468 – 2476. DOI:10.1177/13506501221080282.

22 Roy S., Saha U.K. (2015) Wind tunnel experiments of a newly developed two-bladed Savonius-style wind turbine. *Appl Energy*.,137, 117–125. DOI:10.1016/j.apenergy.2014.10.022.

23 Jens N.S. (2011) Wind Energy Systems: Optimising Design and Construction for Safe and Reliable Operation. *Woodhead Publishing,* DOI:10.1533/9781857090638.

24 Amirat Y., Benbouzid M.E.H., Bensaker B., Wamkeue R. (2007) Condition Monitoring and ault Diagnosis in Wind Energy Conversion Systems: *A Review in Electric Machines and Drives Conference*. IEMDC '07, IEEE International. DOI:10.1109/IEMDC.2007.383639.

25 Zhang M.X., Ou Y.D., Yuan H.B., Pan J.L., Ma L. (2023) Simulation experiment study on friction and wear of materials under high humidity conditions. *Industrial Lubrication and Tribology,* 75, 6, 672 – 678. DOI:10.1108/ILT-04-2023-0090.

AUTHORS' INFORMATION

Mohammed, Omar A. – MSE, Lecturer, Department of Mechanical Engineering, College of Engineering, University of Mosul, Mosul, Iraq; 55175671700; SCOPUS Author ID: 57212494891; ORCID: 0000-0001-7126-1599; Omar.a.mohammed@uomosul.edu.iq

Mohammed, Sufyan A. – M.E, Lecturer, Department of Mechanical Engineering, College of Engineering, University of Mosul, Mosul, Iraq; SCOPUS Author ID: 57467887400; ORCID:0000-0001-9291-8297; Sufyan.a.mohammed@uomosul.edu.iq

Ghazaly, Nouby M. – PhD, Professor, Technical College, Imam Ja'afar Al-Sadiq University, Baghdad, Iraq; Department of Mechanical Engineering, South Valley University, Qena, Egypt; SCOPUS Author ID: 55175671700; ORCID: 0000-0001-8460-4407; nouby.ghazaly@eng.svu.edu.eg